

# Report on injections

May 16, 2018

## 1 Introduction

We want to examine how well the Hubble constant can be measured by considering one BNS merger and assuming an electromagnetic counterpart has been detected. Hence, the goal of these three injection runs has been the interest of determining the distance of the injected event under the constraint of keeping the network SNR constant.

The main structure of the injections will be presented in the following (a summary in table 1.0.3 can be found below). Note that every run contains 10 injections.

Every parameter not mentioned in table 1.0.3 is fixed to the parameter estimated for GW170817.

### 1.0.1 Run 1

Run 1 can be thought of as a check how strongly the distance error depends on the noise realization in time. The ten events were inserted at times separated by  $\Delta t = 100$ s each. The  $i^{th}$  event was inserted at  $t_0 = 1187007296\text{s} + \Delta t \cdot i$ . The source was placed at a point in the sky where the Fisher formalism gives the smallest distance error. The mathematical formalism to estimate the network's ability to disentangle  $h_+$  and  $h_\times$  developed by Cutler and Flanagan in [1] is described in the following chapter. The sky angles  $\theta$  and  $\phi$  were kept constant, so that the right ascension was varied. For the second half of the run 1, the polarization angle  $\psi$  was allowed to vary. Since the source is almost face-on we don't expect the distance error to vary much for these injections.

### 1.0.2 Run 2

In run 2, various sources were placed at different positions in the sky. in fig. 1 the distribution can be seen. The real event is marked with a cross. The points chosen with  $\epsilon_D$  minimal are marked with a triangle. The points chosen with the function  $\xi$ , which characterized comparable SNR are labeled with a colored star.

$$\xi = \frac{|\rho_L - \rho_V|}{|\rho_L + \rho_V|} + \frac{|\rho_L - \rho_H|}{|\rho_L + \rho_H|} + \frac{|\rho_H - \rho_V|}{|\rho_H + \rho_V|} \quad (1)$$

The source marked as a white star, was chosen with the distance error calculated with the Fisher matrix being minimal (The Fisher matrix for the parameters  $\mathcal{M}, \cos(\iota), D, \alpha, \delta, \psi, t_c, \phi_c$ ).

Run 1. Injection	0	1	2	3	4	5	6	7	8	9
$\Delta t$	0	100	200	300	400	500	600	700	800	900
$\psi$	1.16420	1.16420	1.16420	1.16420	1.16420	0	$\pi/6$	$\pi/3$	$2\pi/3$	$5\pi/6$

Table 1: Injection parameters for run 1

Run 2. Injection	0	1	2	3	4	5	6	7	8	9
$\Delta t$	0	100	200	300	400	500	600	700	800	900
Comment	real event	$\epsilon_D$ min.	$\rightarrow$	$\rightarrow$	$\rightarrow$	SNR	$\rightarrow$	$\rightarrow$	$\rightarrow$	Fisher min.

Table 2: Injection parameters for run 2

Run	Variable parameters	Fixed parameters different from real event
1 Inj. 0 – 4	$t_0$	$\theta, \phi, d$
1 Inj. 5 – 9	$t_0, \psi, d$	$\theta, \phi$
2	$\theta, \phi, d$	
3	$\cos(\iota), d$	$\theta, \phi, t_0$

Table 3: Summary of the three runs

### 1.0.3 Run 3

In run 3, the sky position was again fixed to minimal  $\epsilon_D$ . For this run,  $t_0$  was also constant. The two variables were  $v = \cos(\iota)$  and  $d$ .  $v$  varied linearly between 0 and  $\pi/2$ .

All the values which are not further specified are fixed to the estimated values of the real event.

## 1.1 The Fisher matrix formalism

A very useful matrix is the definition in [1]:

$$\kappa^{ab} = \frac{\int_0^\infty f^{-7/3} [S_n^{-1}]^{ab} df e^{2\pi f i(\tau_b - \tau_a)}}{\int_0^\infty f^{-7/3} S_{n,aver}^{-1} df} \quad (2)$$

In our case of uncorrelated noise in the detectors it is diagonal.  $S_{n,aver}^{-1} = n_{(a)}^{-1} \sum_a S_{n,a}^{-1}$  with  $n_{(a)}$  denoting the number of detectors.

Cutler & Flanagan introduce the matrix  $\Theta$  which measures how well the detector network is able to differentiate between the two polarizations.

$$\Theta^{AB} = \sum_{a,b} F_a^A F_b^B \kappa^{ab} \quad (3)$$

In order for  $\Theta$  to be diagonal  $\psi$  is redefined:  $\psi \rightarrow \bar{\psi} = \psi + \Delta\psi$ . Because of the behavior under rotations of  $F_+$  and  $F_\times$

$$\begin{pmatrix} \bar{F}_+ \\ \bar{F}_\times \end{pmatrix} = \begin{pmatrix} \cos(2\Delta\psi) & \sin(2\Delta\psi) \\ -\sin(2\Delta\psi) & \cos(2\Delta\psi) \end{pmatrix} \begin{pmatrix} F_+ \\ F_\times \end{pmatrix} \quad (4)$$

$\Theta$  transforms as

$$\bar{\Theta} = R(2\Delta\psi) \Theta R(-2\Delta\psi) \quad (5)$$

If one chooses the new  $\bar{\psi}$  such that  $\tan(4\Delta\psi) = \frac{2\Theta^{+\times}}{\Theta^{++} - \Theta^{\times\times}}$ ,  $\Theta$  is diagonal.

$\epsilon_D$  and  $\sigma_D$  describe the matrix  $\Theta$  in its Eigenbasis:

$$\Theta_{diag} = \sigma_D \begin{pmatrix} 1 + \epsilon_D & 0 \\ 0 & 1 - \epsilon_D \end{pmatrix} \quad (6)$$

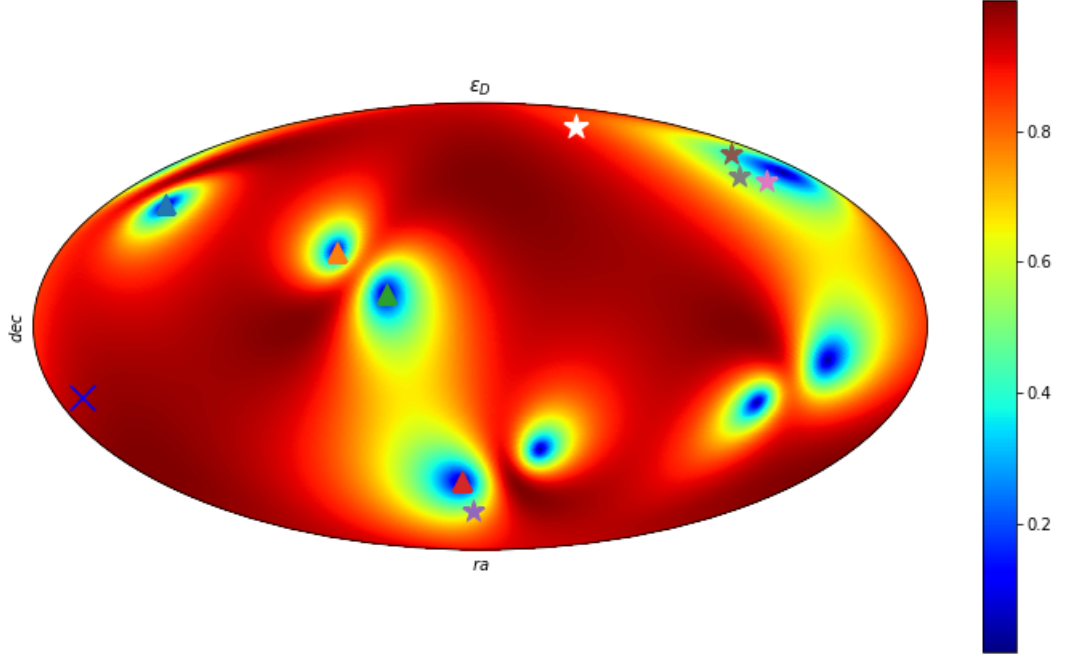


Figure 1:  $\epsilon_D$  at  $t = 1187007296s$

where  $0 \leq \epsilon_D \leq 1$

Note that even though  $F_+$  and  $F_\times$  depend on  $\psi$ , the matrix  $\theta$  is by construction independent of  $\psi$ . For simple examples the meaning of  $\theta$  becomes clear. If one of the polarization is close to zero (for every detector), then one Eigenvalue of  $\theta$  approaches zero. Hence,  $\epsilon_D$  has to be close to unity. But at points where only one polarization is measured, one cannot expect a good estimate on the inclination. This implies also a not well constrained distance.

In the opposite case, where for one detector  $F_+$  is very high and  $F_\times$  low and for the other detectors vice versa, the polarizations are well measured each and we expect the distance to be better constrained. Since the Eigenvalues of  $\theta$  are almost identical,  $\epsilon_D$  is close to zero. In conclusion, one should expect the distance error to be proportional to some function which increases with increasing  $\epsilon_D$ .

In order to identify the point in the sky, which gives a good estimate on the distance, we use the Fisher matrix formalism. Denoting  $\tilde{\theta}$  the real parameters, in [2]  $h(\theta)$  is expanded in the SNR  $A := \sqrt{(h(\tilde{\theta})|h(\tilde{\theta}))}$ . Then the first order of the error in the parameters  $\theta_j^{ML}$  and  $\theta_k^{ML}$  is given by:

$$\langle \theta_j^{ML} \theta_k^{ML} \rangle_n = [(\partial_{\theta_j} h | \partial_{\theta_k} h)]^{-1} = [(h_j | h_k)]^{-1} \quad (7)$$

The second equality is simply a different notation. The inverse of the right hand side is called the Fisher matrix:

$$\mathcal{F}_{jk} = (\partial_{\theta_j} h | \partial_{\theta_k} h) \quad (8)$$

The diagonal elements of  $[\mathcal{F}_{jk}]^{-1}$  give the variance  $\Delta\theta_i^2 = \langle \theta_i^2 \rangle - \langle \theta_i \rangle^2$  of the parameter  $\theta_i$ . The off diagonal terms give the correlations between the parameters.

Following this formalism, using the Markovic approximation, meaning that the skyposition is precisely known and assuming Gaussian errors, [1] gives the behavior for the distance error

$$\frac{\Delta D^2}{D^2} = \frac{8D^2}{r_0^2} \frac{1 + v^2 - \epsilon_D \cos(4\bar{\psi})(1 - v^2)}{2\sigma_D(1 - \epsilon_D^2)(1 - v^2)^2} \quad (9)$$

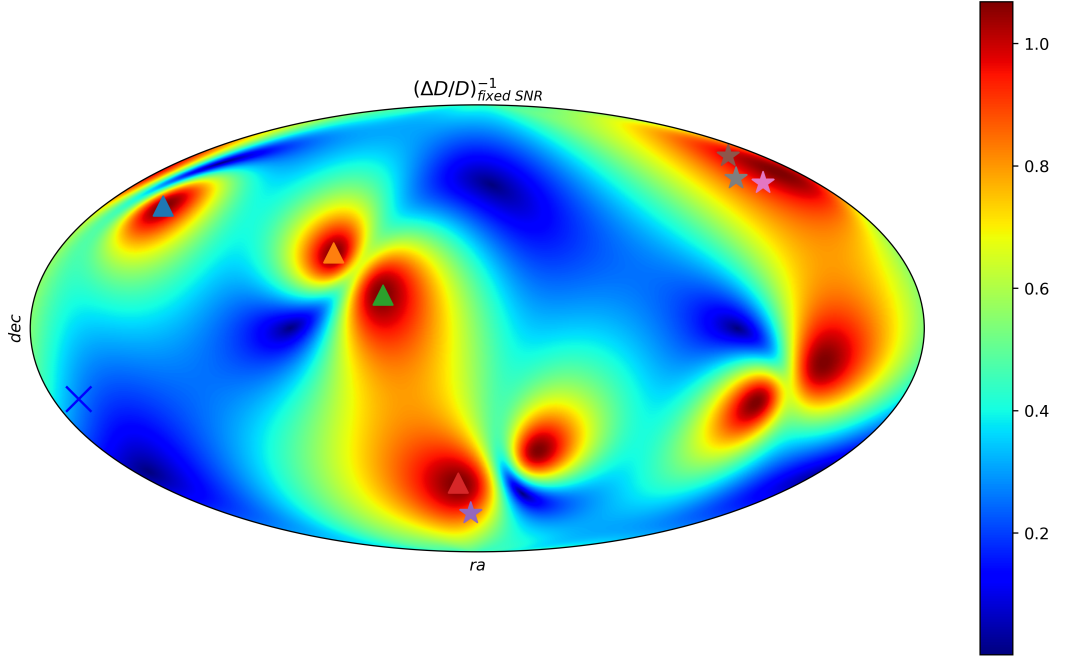


Figure 2: Inverse of the relative distance error for fixed SNR

where  $\sigma$  and  $\epsilon_D$  were introduced in eq. 6.  $r_0 = \rho_0 D$ :

$$\rho_0^2 = \langle \tilde{h}_0, \tilde{h}_0 \rangle_S = 4 \int_0^\infty \frac{|\tilde{h}_0|^2}{S_{n,aver}} df \quad (10)$$

$\rho_0$  can be considered as the SNR if the source would be face-on ( $v = \pm 1$ ) and directly overhead of one detector. It turns out that  $\sigma_D \propto \rho$ , so that the distance error is proportional to  $\rho^{-1}$  as one expects:

$$\rho^2 = \rho_0^2 \sigma_D \left( \frac{(1+v^2)^2}{4} + v^2 + \epsilon_D \frac{(1-v^2)^2}{4} \cos(4\bar{\psi}) \right) \quad (11)$$

Additionally, there are two divergences, one for  $v \rightarrow 1$  and the other for  $\epsilon_D \rightarrow 1$ .

Cutler and Flanagan explain in [1] that the first divergence is due to the breakdown of the Fisher matrix formalism, since the derivatives with respect to distance and inclination become proportional and hence, the determinant of  $\mathcal{F}$  vanishes. This can only be resolved by going to higher orders.

The other divergence of  $\epsilon_D \rightarrow 1$  they claim is a real one, due to the network properties of not being able to disentangle between  $h_+$  and  $h_\times$ .

In the scenario considered, we want to keep the SNR constant, since the errors on the estimated parameters are decreasing with increasing SNR. So eq. 9  $r_0$  is replaced with eq. 11.

$$\frac{\Delta D^2}{D^2} = \frac{\left( \frac{(1+v^2)^2}{4} + v^2 + \epsilon_D \frac{(1-v^2)^2}{4} \cos(4\bar{\psi}) \right) (1 + v^2 - \epsilon_D \cos(4\bar{\psi})(1 - v^2))}{(1 - \epsilon_D^2)(1 - v^2)} \quad (12)$$

The predicted relative distance errors for nearly face-on binaries for a SNR ( $\rho \approx 30$ ) are of order one (drawn in 2), so clearly, an overestimate compared with the errors given by actual events. As mentioned earlier, the Gaussian approximation breaks down.

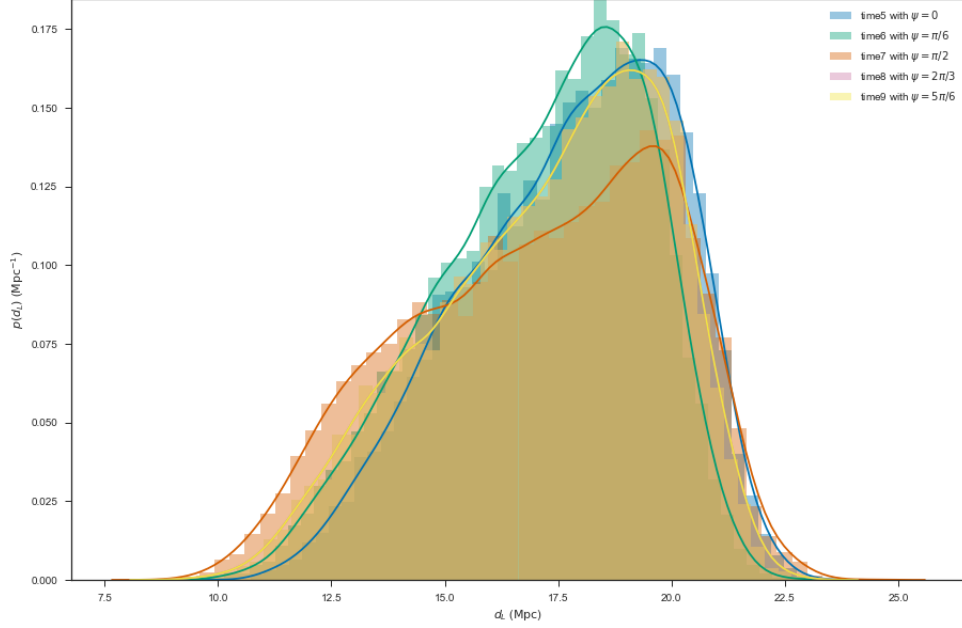


Figure 3: Posterior on distance of run 1, injections 1 – 4

## 1.2 Beyond Gaussian Approximation

In order to lift the degeneracy between distance and inclination Cutler and Flanagan provide a PDF on the relative distance  $\mathcal{D} = \frac{D}{D_0}$  in [1] where  $D_0$  is the distance maximizing the likelihood. The effects between  $D$  and  $v$  are treated beyond linear order.

$$p(v, \mathcal{D}) = \mathcal{N} \mathcal{D}^2 \exp \left\{ -\frac{1}{2\Delta_1^2} \left( \frac{v}{\mathcal{D}} - v_0 \right)^2 - \frac{1}{2\Delta_2^2} \left[ \frac{1+v^2}{2\mathcal{D}} - \frac{1+v_0^2}{2} \right]^2 \right\} \Theta(\mathcal{D}) \Theta \left( \frac{D_{max}}{D_0} - \mathcal{D} \right) \Theta(1-v^2) \quad (13)$$

where  $\mathcal{N}$  is a normalization constant,  $\Theta$  is the step function and the definition:

$$\Delta_1 = \frac{D_0}{r_0} \sqrt{\frac{1 + \epsilon_D \cos(4\bar{\psi})}{\sigma_D (1 - \epsilon_D^2)}} \quad \Delta_2 = \frac{D_0}{r_0} \sqrt{\frac{1 - \epsilon_D \cos(4\bar{\psi})}{\sigma_D (1 - \epsilon_D^2)}}$$

$D_{max}$  is a cutoff distance, which has to be introduced in order to make eq. 13 normalizable. The physical meaning of  $D_{max}$  is that distant sources are not detectable.

## 2 Results

### 2.1 Run 1

Since we are interested in the distance uncertainty, we will take a look at the posterior samples of  $d$ . They can be seen in fig. 3.

We can see that the different noise realizations don't affect the estimated distance strongly. Still, taking a closer look at injection 2, it has a much more irregular shape than the other PDFs.

### 2.2 Run 2

The distance posterior is plotted below.

Run 1. Injection	0	1	2	3	4	5	6	7	8	9
Network SNR	-	32.8	33.9	34.3	33.3	33.4	32.8	32.8	33.9	-
$\Delta D$	-	2.34	2.78	2.18	2.2	2.3	2.26	2.84	2.5	-

Table 4: Summary of results for run 1

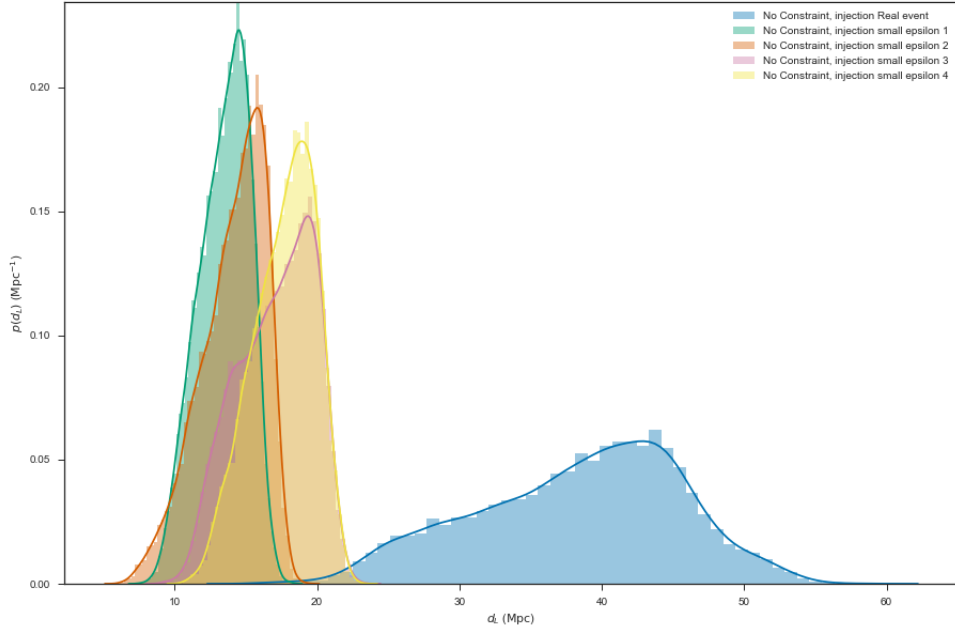


Figure 4: Posterior on distance of run 2, injections 0 – 4

Since, we are more interested in the relative distance error, let's take a look at the posterior of the relative distance in fig. 6 and 7.

Note that the first event of run 2 had a sky position equal to the one of the real event. One sees that all PDFs are narrow around the mean value of the estimated distance. To quantify this statement we can look at the relative distance error  $\Delta D/D = std(D)/average(D)$ .

The main results are summarized in table 2.3

Which is in decrease of distance error in the best case (injection 4) of 37% and in the worst case (injection 9) of 10%. One can see that eq. 12 overestimated the errors for  $v \approx 1$ . If one would ignore this and take the ratios of the relative distance errors in the sky one finds

$$\frac{(\Delta D/D)_{real\ event}}{(\Delta D/D)_{inj01}} \approx \frac{(\Delta D/D)_{real\ event}}{(\Delta D/D)_{inj02}} \approx \frac{(\Delta D/D)_{real\ event}}{(\Delta D/D)_{inj03}} \approx \frac{(\Delta D/D)_{real\ event}}{(\Delta D/D)_{inj04}} \approx 4 \quad (14)$$

which is clearly overstating the improvement we see on the distance error. Therefore, it is useful to use the PDF on distance and inclination given in 13. The comparison between the prediction and the inferred inclination and distance are plotted in fig. 8 and fig. 9 for the real event and in fig. 10 and fig. 11 for injection 4. The SNR for Livingston, Hanford and Virgo were for the real event (26, 19, 3) and for injection 4 (20, 17, 20) respectively. The high SNR in Virgo doesn't break the degeneracy between  $D$  and  $v$ .

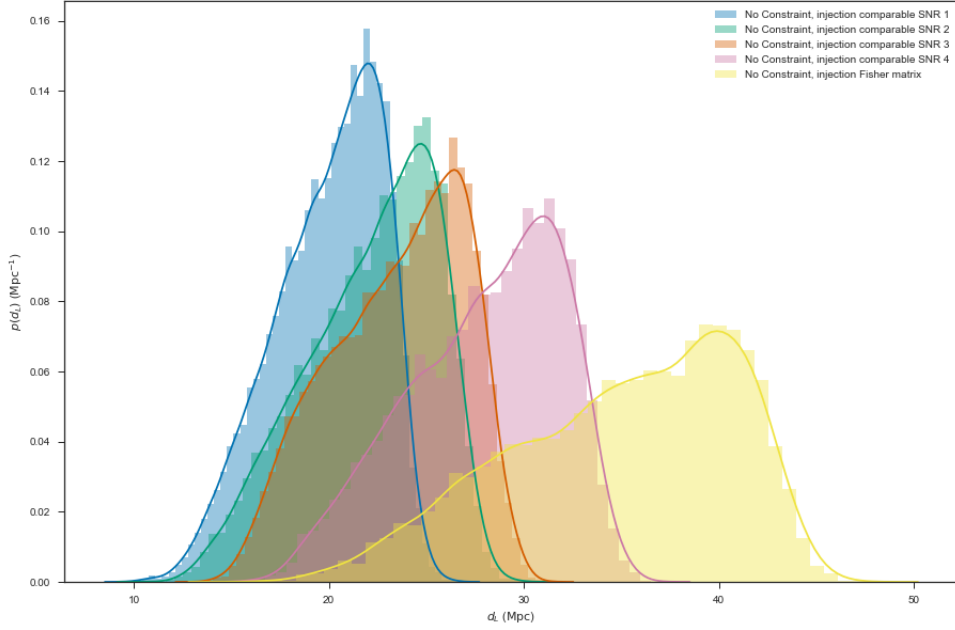


Figure 5: Posterior on distance of run 2, injections 5 – 9

Run 2. Injection	0	1	2	3	4	5	6	7	8	9
Network SNR	32.55	33.58	33.74	32.15	33.35	33.49	33.92	33.35	33.27	34.21
$\frac{\Delta D}{D}$	0.19	0.13	0.16	0.15	0.12	0.14	0.15	0.14	0.14	0.17

Table 5: Summary of results for run 2

### 2.3 Run 3

One would expect for fixed SNR better distance constraints for face-on binaries, but very surprisingly table 2.3 shows that the face-off injection (injection 9) gives by far the best distance constraints.

## References

- [1] Curt Cutler and Eanna E Flanagan. Gravitational waves from merging compact binaries: How accurately can one extract the binarys parameters from the inspiral waveform? *Physical Review D*, 49(6):2658, 1994.
- [2] Michele Vallisneri. Use and abuse of the fisher information matrix in the assessment of gravitational-wave parameter-estimation prospects. *Physical Review D*, 77(4):042001, 2008.

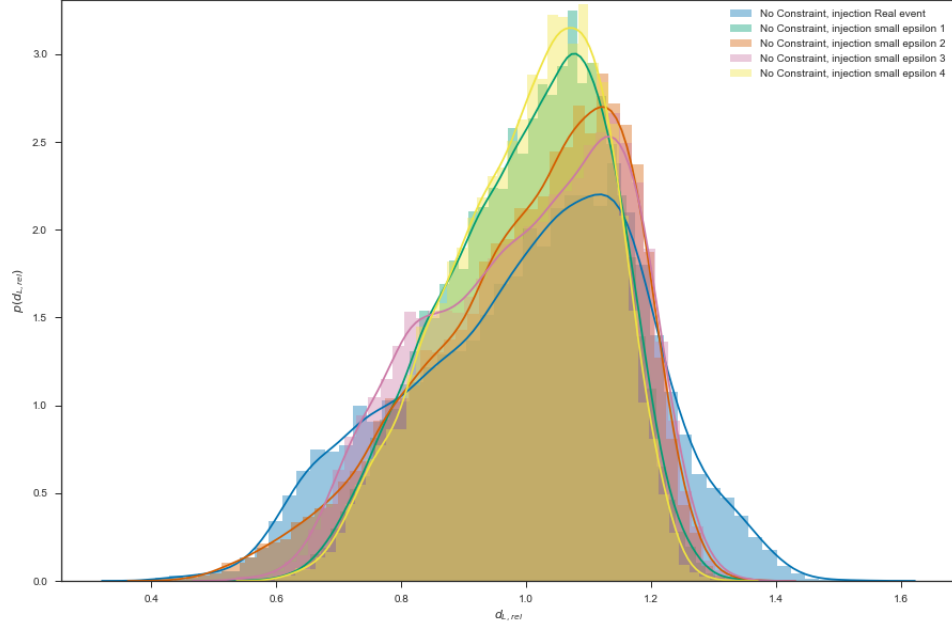


Figure 6: Posterior on the relative distance of run 2, injections 0 – 4

Run 3. Injection	0	1	2	3	4	5	6	7	8	9
Network SNR	34.76	33.21	33.2	33.21	33.19	33.17	33.15	33.04	-	32.63
$\frac{\Delta D}{D}$	0.13	0.15	0.15	0.15	0.14	0.13	0.12	0.17	-	0.064

Table 6: Summary of results for run 3



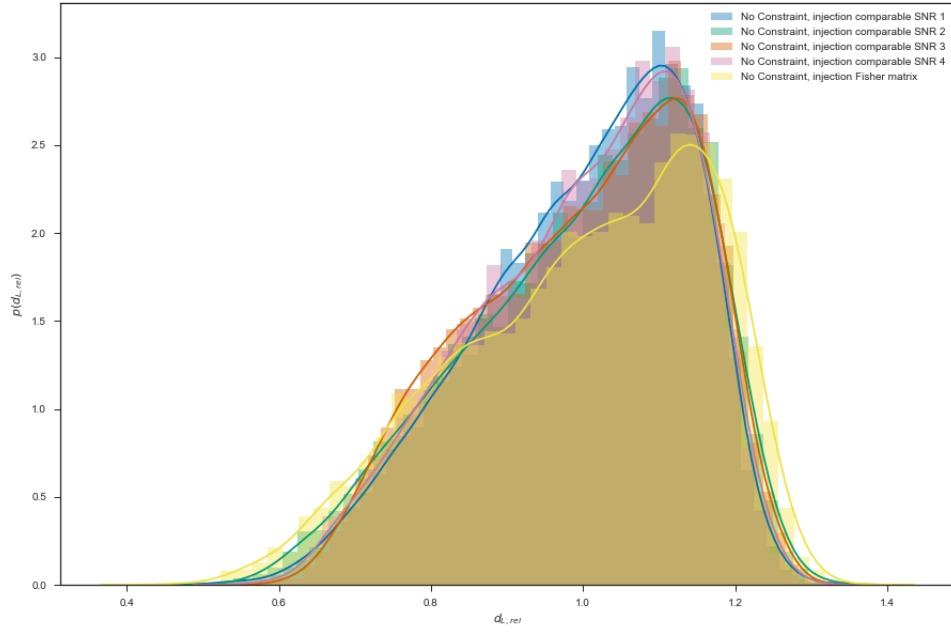


Figure 7: Posterior on the relative distance of run 2, injections 5 – 9

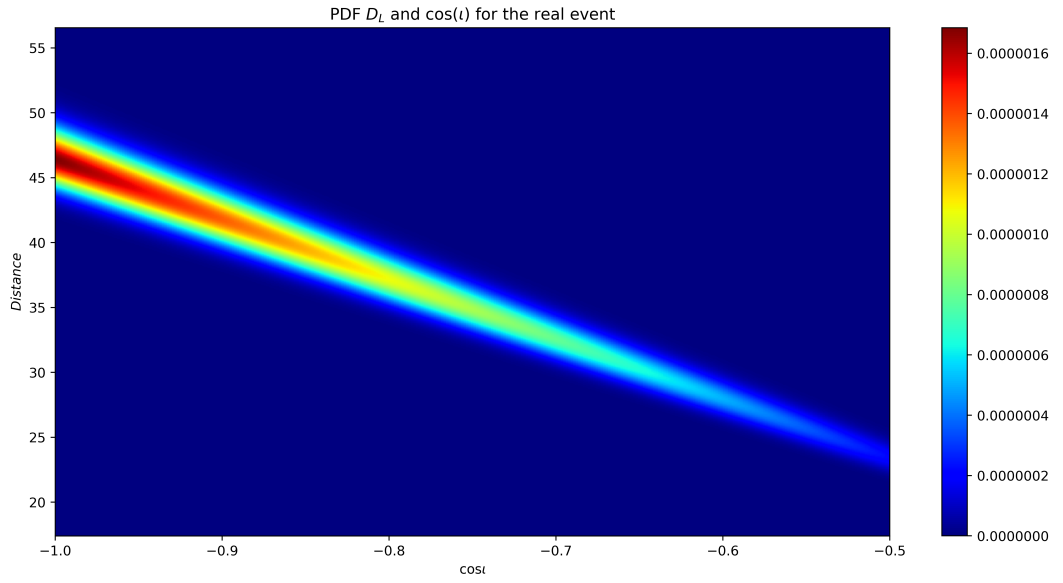


Figure 8: Theoretical PDF for the real event, with fixed sky position

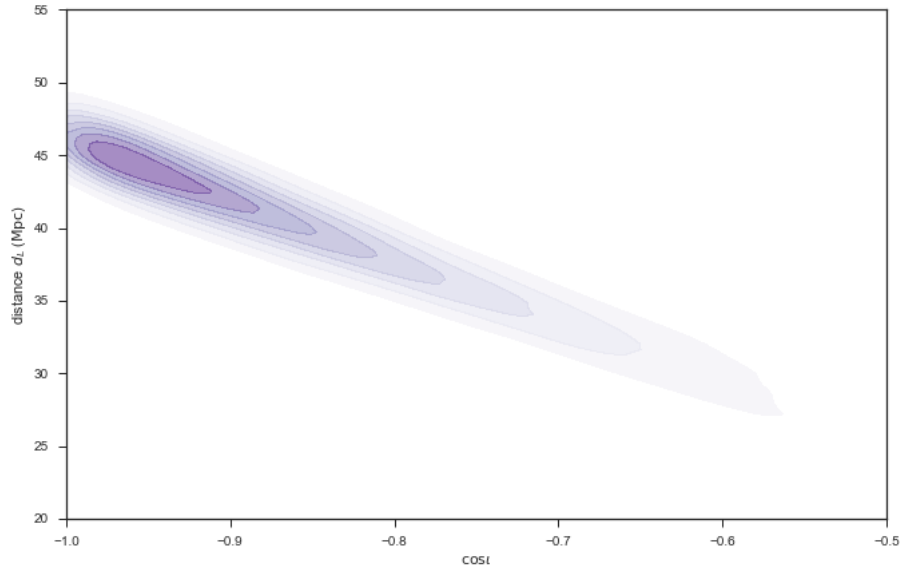


Figure 9: PDF for the real event, with fixed sky position

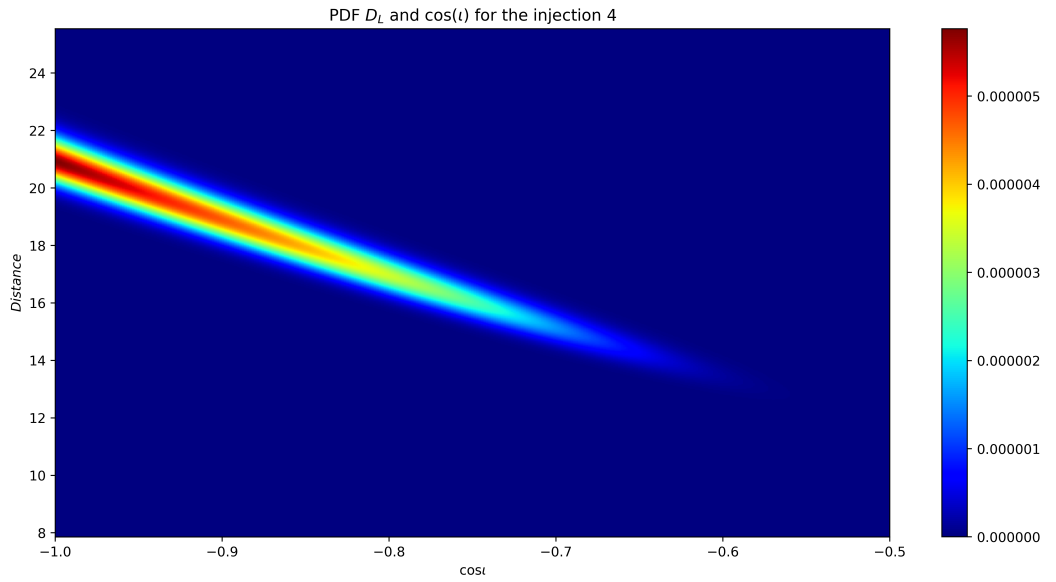


Figure 10: Theoretical PDF for injection 04

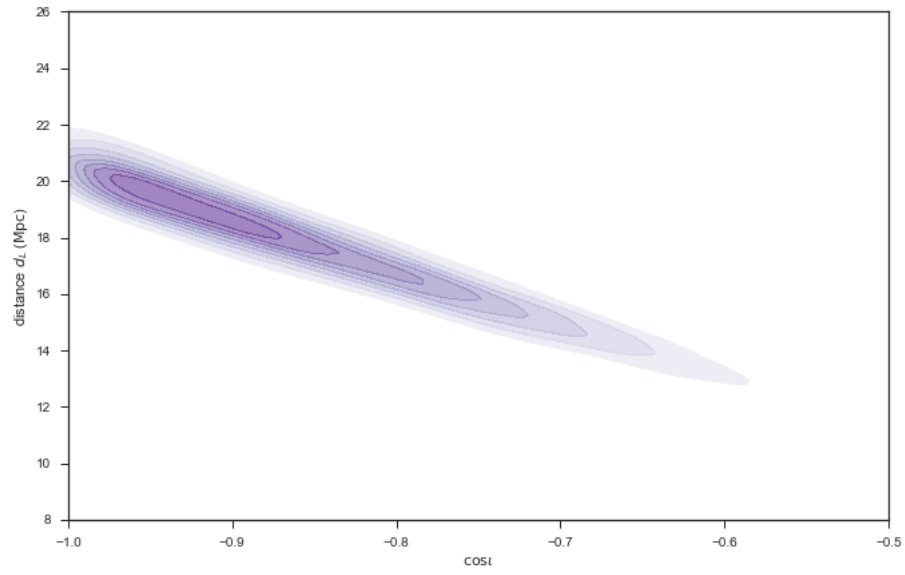


Figure 11: PDF for injection 04